PETROLOGICAL AND GEOCHEMICAL INVESTIGATIONS OF THE GRANITE BASEMENT IN THE CHICXULUB PEAK RING: IMPLICATIONS FOR THE YUCATÁN TARGET ROCK. J. -G. Feignon[1], S. J. de Graaff[2,3], L. Ferrière[4], P. Kaskes[2,3], T. Déhais[2,3], S. Goderis[2], P. Claeys[2], and C. Koeberl[1], [1]Department of Lithospheric Research, University of Vienna, Althanstrasse 14, A-1090 Vienna, Austria (jean-guillaume.feignon@univie.ac.at), [2]Research Unit: Analytical, Environmental & Geo-Chemistry, Department of Chemistry, Vrije Universiteit Brussel, AMGC-WE-VUB, Pleinlaan 2, 1050 Brussels, Belgium, [3]Laboratoire G-Time, Université Libre de Bruxelles, Av. F.D. Roosevelt 50, 1050 Brussels, Belgium, [4]Natural History Museum, Burgring 7, 1010 Vienna, Austria.

Introduction: In 2016, the joint International Ocean Discovery Program (IODP)-International Continental Scientific Drilling Program (ICDP) Expedition 364 drilling recovered an 829 m long core, between 505.7 and 1334.7 mbsf (meters below sea floor), in the Chicxulub impact structure peak ring. Approximately 600 m of near continuous crystalline basement were sampled, forming the "lower peak ring" section [1]. The bulk of the basement consists of pervasively deformed, fractured, and shocked granite [2]. It is the first time that a continuous crystalline basement unit is recovered within the Chicxulub structure. As granites are a major component of the impactites recovered from the peak ring, investigating a large set of samples of such rocks offers a unique opportunity to better characterize petrology, chemistry, sources of the granite, and provide a more detailed understanding how it was affected by the impact event and, more generally, refine the Yucatán peninsula basement geology.

Material and Methods: Forty-one granite samples were selected at regular intervals between 745.1 and 1334.7 mbsf. To assess any chemical variation related to petrographic textures or position throughout the drill core, samples were taken from: (1) the main granite unit (i.e., continuous granite interval larger than one meter in thickness, n = 33), (2) granite clasts within impact melt rock (n = 4), (3) granite breccias (n = 2), and (4) aplites (n = 2). Petrographic investigations on polished thin sections (mineralogy, texture, and shock metamorphic features) were carried out using optical and scanning electron microscopy. Major and trace element mapping was performed on 20 granite samples by micro X-ray fluorescence (μXRF). Whole-rock major and trace element concentrations were measured using bulk X-ray fluorescence (XRF) and instrumental neutron activation analysis. Finally, Sr-Nd isotopic analytical work was performed on 14 granites and two granite clasts out of the 41 aforementioned samples using thermal ionization mass spectrometry.

Results: Granite (main unit) and granite clast samples mainly consist of equigranular coarse-grained, holocrystalline and phaneritic leucogranite (Fig. 1A). The bulk mineral assemblage is mainly composed of orange to brownish K-feldspar (orthoclase, ~25–50 vol%), plagioclase (~15–35 vol%), quartz (~15–35 vol%) and, to a lesser extent, biotite (generally 1–5 vol%). The grain size varies from ~0.5 to 4 cm for K-feldspar, plagioclase, and quartz, and from ~0.1 to 1 cm for biotite. The main accessory minerals are muscovite, (fluor)apatite, titanite, secondary epidote (piemontite) located in cataclasite areas or associated with calcite veins, zircon, (titano)magnetite, and allanite, representing less than 1 vol% of the mineral assemblage and grain size <0.5 mm. Alteration is pervasive, as evidenced by secondary epidote mineralization, likely due to hydrothermal alteration, sericitization of plagioclases, and common chloritization of biotite (see also [3]). The granite unit is pervasively deformed to different degrees from one sample to another, with occurrence of pre-impact ductile mineral deformation, and abundant syn-impact fracturing, shearing, cataclasite veins cross-cutting the granite, and shock metamorphic features in rock-forming minerals (Fig. 1B), with estimated shock pressures experienced by the granite between ~16 and 18 GPa (see details in [2]).

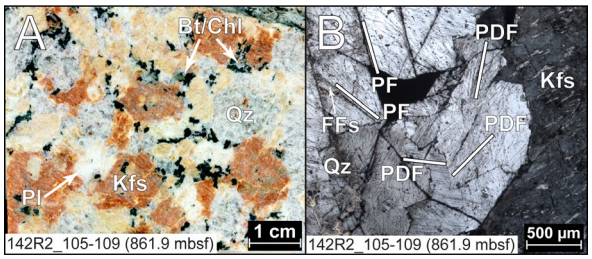

Figure 1. *A) Coarse-grained granite exhibiting the typical paragenesis: K-feldspar (Kfs), quartz (Qz), plagioclase (Pl), biotite (Bt), and chlorite (Chl). B) Granite photomicrograph (cross-polarized light). Quartz is shocked with at least two sets of PFs (with FFs) and several sets of PDFs.*

Two of the investigated samples consist of monomict granite breccia made of ~0.5 mm mineral clasts (mainly quartz and K-feldspar with rare occurrence of biotite). The matrix (~45–50 vol%) is made of brecciated quartz, K-feldspar, and, to a lesser extent, calcite. The clastic breccia shows no signs of melting.

Aplites have fine-grained (mean mineral size < 1 mm), homogeneous, equigranular texture. Paragenesis consists of K-feldspar, quartz, and plagioclase, whereas biotite is nearly absent. Shock features in the form of planar fractures (PFs) and planar deformation features (PDFs) are observed in quartz grains.

Major element abundances in the investigated samples show broadly similar patterns with few exceptions, independently of the sample type (granite, granite clast, granite breccia, or aplite) or the depth in the drill core, and represent the most evolved lithology compared to pre-impact dikes, suevites, and impact melt rocks. Nearly all granites have a composition of 69.7–77.5 wt.% SiO_2, and 6.85–9.38 wt.% total alkalis ($Na_2O + K_2O$) (Fig. 2). Two samples display a monzo-granitic composition. The sample suite spreads between the calc-alkaline and the high-K calc-alkaline series. The Al_2O_3 and CaO contents decrease (16.06–11.55 and 3.04–0.70 wt.%, respectively) with increasing SiO_2 contents. The outlier compositions can be explained either by the presence of certain minerals (e.g., biotite, titanite, or apatite) or of calcite-filled fractures, as also noted in μXRF mapping. The investigated samples are metaluminous to weakly peraluminous.

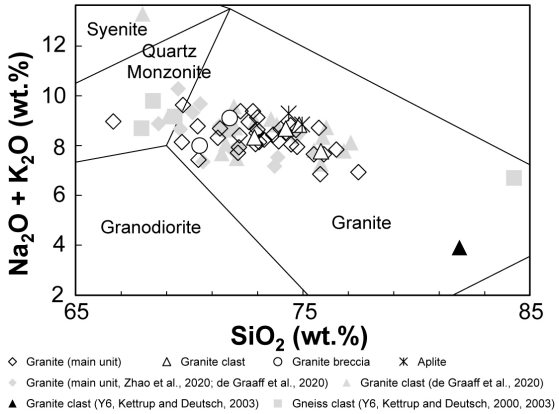

Figure 2. *Total alkalis versus SiO_2 (TAS) diagram.*

Trace element contents in granites display similar patterns with enriched compositions relative to CI-chondritic values. Fluid-mobile elements, such as Ba and U, are highly enriched, whereas nearly all samples show a depletion in Pb. Additionally, Nb and Ta show a relative depletion, while Zr and Hf show a moderate enrichment, relative to neighboring trace elements, a pattern typical of arc-type magmatism [4]. No pronounced positive or negative Eu anomalies are present, while Yb shows a negative anomaly relative to Er and Y ($Yb^* = 0.81 \pm 0.30$).

Trace element compositions of the granite clasts, granite breccias, and aplites do not show significant differences, with only some enrichment or depletion for a given element. One granite breccia is enriched in Pb, which may be explained by the presence of a Pb-bearing phase (e.g., sulfide minerals).

Additionally, the samples are characterized by high Sr/Y and $(La/Yb)_N$ ratios, and low Y and Yb contents, which are typical for adakites. However, other criteria (such as Al_2O_3 and MgO contents, Mg#, K_2O/Na_2O ratio, Ni concentrations, etc.) do not match the adakite definition [5].

The present-day $^{87}Sr/^{86}Sr$ ratios show a distinct variability and can be divided in two separate groups: (1) the less radiogenic "group 1" (n = 10, 0.70798–0.71023) and (2) the more radiogenic "group 2" (n = 6, 0.71165–0.71371) samples. In contrast, current $^{143}Nd/^{144}Nd$ ratios display limited variations (0.512410–0.512484) and $(\varepsilon Nd)_{t=0}$ values plot in a narrow range between -4.4 and -3.0 for all the investigated samples (Fig. 3).

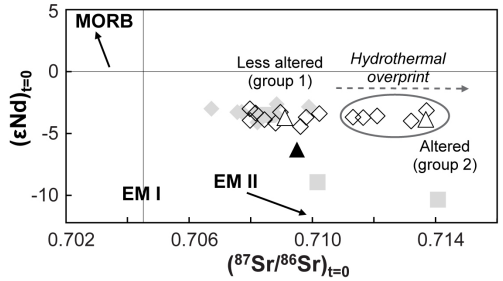

Figure 3. *Present-day εNd and $^{87}Sr/^{86}Sr$. Legend is the same as in Fig. 2.*

Discussion and Conclusions: The investigated samples are chemically relatively homogeneous with only limited variations in composition, and should be termed as high-K, calc-alkaline granites. Textural variations do not significantly affect the composition. The Al_2O_3 content and the absence of Eu anomaly suggest that these granites represent intrusions rather than cumulates. Trace element compositions are consistent with an emplacement within an arc setting, during one magmatic event, with a moderately evolved crustal component involved in the melting process, as suggested by Sr-Nd isotopic data of "group 1" granites. Enrichments in Ba, Rb, and U, associated with the high $^{87}Sr/^{86}Sr$ of "group 2" granites may reflect post-impact hydrothermal alteration [3]. In general, our results are consistent with previous work on a more limited set of samples [6,7] and further support that the investigated granite unit could be related to arc magmatism in the Maya Block during the closure of the Rheic ocean and Pangea assembly in the Carboniferous [6]. Importantly, a similar granite composition was not found in any previous drill cores recovered within the Chicxulub impact structure [8,9].

Acknowledgements: Thanks to ECORD, IODP-ICDP, the Yucatán Government, and Universidad Nacional Autónoma de México for funding the drilling. University of Vienna doctoral school, FWO-Flanders, BELSPO, and VUB Strategic Research Program supported this research.

References: [1] Morgan J. V. et al. (2016) *Science, 354,* 878–882. [2] Feignon J. -G. et al. (2020) *Meteorit. Planet. Sci., 55*, 2206–2223. [3] Kring D. A. et al. (2020) *Sci. Adv., 6,* eaaz3053. [4] Pearce J. A. (1984) *J. Petrol., 25,* 956–983. [5] Moyen J. -F. (2009) *Lithos, 112*, 556–574. [6] Zhao J. et al. (2020) *Gondwana Res., 82*, 128–150. [7] de Graaff S. J. et al. *GSA Bull.* (in revision). [8] Kettrup B. et al. (2000) *Meteorit. Planet. Sci., 35*, 1229–1238. [9] Kettrup B. and Deutsch A. (2003) *Meteorit. Planet. Sci., 38*, 1079–1092.